On the Multi-Depot Electric Bus Vehicle Scheduling Problem with Time Windows: An Exact Continuous-Time Formulation

Dimitrios Rizopoulos*[1] and Konstantinos Gkiotsalitis[2]

[1]Ph.D. Candidate, Department of Transportation Planning and Engineering, School of Civil Engineering, National Technical University of Athens, Zografou Campus, 9, Iroon Polytechniou str, 15780, Athens, Greece
[2]Associate Professor, Department of Transportation Planning and Engineering, School of Civil Engineering, National Technical University of Athens, Zografou Campus, 9, Iroon Polytechniou str, 15780, Athens, Greece

Short summary

The electrification of bus fleets is a systemic transition that goes beyond the acquisition of vehicles and charging infrastructure, requiring new operational practices and planning approaches for effective implementation. At the tactical level planning, vehicle scheduling must at least consider depot, charging, and time-window constraints, as well as electric-vehicle-specific characteristics such as battery capacity, energy consumption, and charging power rates. This study extends the Electric Bus Multi-Depot Vehicle Scheduling Problem with Time Windows (EB-MD-VSP-TW) by introducing continuous-time modeling at charging stations, aiming to improve the fidelity of charging operations in the calculated solutions. The proposed model is evaluated using both synthetic instances and real-world bus lines from Athens, Greece. Given the continuous-time EB-MD-VSP-TW formulation, a heuristic solution approach is also proposed to produce feasible schedules for a set of four operational bus lines.
Keywords: electric buses; vehicle scheduling; public transport; operations research applications.

1 Introduction

The transition from conventional to electric bus fleets is a system-wide change that affects strategic, tactical, and operational planning (Lipman, 2025). Strategic decisions on charging infrastructure, fleet composition, and line design directly shape the feasibility and cost of downstream scheduling decisions (Davatgari et al., 2024). At the tactical level, vehicle scheduling must account for depot and time-window constraints together with battery capacity, energy consumption, charging duration, and charger availability.

These planning complexities are further intensified by climate and environmental policy. Transport remains a major source of greenhouse gas emissions in the European Union, and urban road transport contributes substantially (Pelletier et al., 2019). Initiatives such as the European Green Deal and Fit for 55 have increased pressure on public transport authorities to decarbonize operations, while transit agencies are moving from pilot projects toward broader zero-emission bus deployment (Lu et al., 2023). Despite these efforts, decarbonization of transport still includes major implementation challenges, including procurement of environmentally friendly vehicles, existing infrastructure adaptation, and operational reorganization (Rogge & Goedeking, 2024). Among these challenges, tactical scheduling also emerges as a critical bottleneck, bringing the Vehicle Scheduling Problem and its variants to the forefront.

In the research domain, the Vehicle Scheduling Problem (VSP) is one of the main methodological tools for tactical scheduling under fixed timetables and route-feasibility constraints (Orloff, 1976; Bodin, 1990). Work over the last few decades has introduced multi-depot formulations and richer operational realism, including time windows and waiting costs, solved with exact methods such as branch-and-bound and column generation (Carpaneto et al., 1989; Desaulniers et al., 1998). Electrification necessitates the extension of the VSP framework by adding battery and charging constraints, motivating Electric Bus (EB) scheduling formulations that explicitly model duty feasibility and charging operations (Jiang & He, 2022; Yao et al., 2020).

While Gkiotsalitis et al. (2023) formulated and strengthened the EB-MD-VSP-TW, showing that exact methods can solve medium-sized instances, a parallel research stream tackles the compu-

tational burden of realistic scheduling models through heuristics and hybrid methods. Even in classical large-scale VSP (without electric bus features), studies distinguished exact methods for benchmarking from heuristics for operational-scale applications (Eliiyi et al., 2009). Under electrification, this distinction becomes more pronounced because charging feasibility expands the combinatorial search space. Recent work therefore uses heuristic and hybrid methods, including genetic algorithms, reinforcement learning, and machine-learning-assisted column generation, to produce high-quality solutions for large electric bus scheduling instances (Gerbaux et al., 2025). Overall, exact methods remain important as benchmarks, while heuristics increasingly determine what is computationally tractable in practice.

Within this context, this study extends the EB-MD-VSP-TW by introducing continuous-time modeling at charging stations to improve charging-time fidelity relative to discrete-time approximations. Because this addition increases computational difficulty, a heuristic solution approach is also proposed that leverages the exact formulation within a tractable decomposition framework. The methodology is evaluated on reusable synthetic instances (Carpaneto et al., 1989; Desaulniers et al., 1998; Gkiotsalitis et al., 2023; Wang et al., 2021) and real-world bus lines from Athens, Greece.

2 Methodology

The current section presents the methodological framework of the proposed research work. The following assumptions are made. We assume a day-ahead fixed set of service trips with predefined start/end times and time windows that must be covered exactly once within a single-day horizon; a homogeneous electric fleet with deterministic travel times, public transport service durations, deadheading times, and per-distance energy consumption; unit-capacity chargers with uninterrupted continuous charging at constant rate; full charging when a charger is visited. Finally, charging is not directly rewarded or penalized in the objective function, but is selected only when it improves feasibility, or cost through reduced waiting between completing the services.

Fundamental MD-VSP-TW Formulation

This section presents the classical MD-VSP-TW formulation used as the basis for the subsequent proposed developments. The problem is modeled as a multi-commodity flow formulation on a graph $\mathcal{G} = (N, A)$, composed of vehicle-specific subgraphs $\mathcal{G}^k = (N^k, A^k)$ for each vehicle $k \in K$. The set V denotes the service trips, and $V^k \subseteq V$ the trips feasible for vehicle k. For each arc $(i,j) \in A^k$, parameter c_{ij}^k denotes traversal cost and t_{ij}^k denotes travel (deadheading) time. The origin and destination depots of vehicle k are denoted by o_k and d_k, respectively. Binary variable x_{ij}^k indicates whether vehicle k traverses arc (i,j), and continuous variable T_i^k denotes the service start time at node i for vehicle k. Parameter $\tilde{t}_i$ represents the time required to execute trip i, while l_i and u_i are the lower and upper bound of time window within which trip i may be executed. The MD-VSP-TW formulation is given by (1)–(8).

$$\min \quad \sum_{k \in K} \sum_{(i,j) \in A^k} c_{ij}^k x_{ij}^k \tag{1}$$

$$\text{s.t.} \quad \sum_{k \in K} \sum_{i:(i,j) \in A^k} x_{ij}^k = 1 \qquad \forall j \in V \tag{2}$$

$$\sum_{i:(i,j) \in A^k} x_{ij}^k - \sum_{i:(j,i) \in A^k} x_{ji}^k = 0 \qquad \forall j \in V^k,\ \forall k \in K \tag{3}$$

$$\sum_{j:(o_k,j) \in A^k} x_{o_k j}^k = \sum_{i:(i,d_k) \in A^k} x_{i d_k}^k \qquad \forall k \in K \tag{4}$$

$$T_j^k \geq T_i^k + \tilde{t}_i + t_{ij}^k - M(1 - x_{ij}^k) \qquad \forall k \in K,\ \forall (i,j) \in A^k \tag{5}$$

$$l_i \leq T_i^k \leq u_i \qquad \forall k \in K,\ \forall i \in N^k \tag{6}$$

$$x_{ij}^k \in \{0,1\} \qquad \forall k \in K,\ \forall (i,j) \in A^k \tag{7}$$

$$T_i^k \in R_+ \qquad \forall k \in K,\ \forall i \in N^k \tag{8}$$

The objective (1) minimizes total operating cost. Constraint (2) ensures exact trip coverage. Constraint (3) enforces vehicle-wise flow conservation at trip nodes, while (4) guarantees depot-flow consistency for each vehicle. Constraint (5) propagates service start times along selected arcs through a big-M formulation. Constraint (6) enforces trip time windows. Constraints (7) and (8) define the binary and continuous decision-variable domains, respectively.

Extending MD-VSP-TW for Electric Bus Fleets

In contrast to the classical case of MD-VSP-TW, in the EB-MD-VSP-TW, electric buses face battery limitations and non-negligible re-fueling times, so the formulation needs to incorporate charging-station nodes that may be visited during the planning horizon. Figure 1 illustrates this extension of the classical MD-VSP-TW with the additional charger nodes $F_1, \ldots, F_n \in F$.

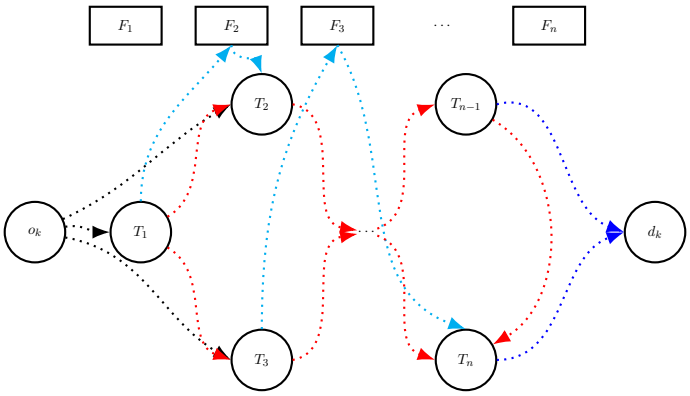


Figure 1: Sub-graph $\mathcal{G}^k = (\mathcal{N}^k, \mathcal{A}^k)$ for vehicle k in the EB-MD-VSP-TW. The $\mathcal{F}_i$ nodes represent charger nodes where optional intermediate charging can be achieved.

Following prior electric vehicle scheduling work (Wang et al., 2021), we include waiting time using variable w_{ij}^k, representing waiting at node j after transition (i,j) when $x_{ij}^k = 1$. The MD-VSP objective function (1) is extended to (9) by adding waiting-time cost.

$$\min \quad \sum_{k \in K} \sum_{(i,j) \in A^k} c_{ij}^k x_{ij}^k + \sum_{k \in K} \sum_{(i,j) \in A^k} \lambda_1 w_{ij}^k \tag{9}$$

The parameter λ_1 weights waiting time. Constraint (10) activates and lower-bounds w_{ij}^k through a big-M formulation.

$$w_{ij}^k \geq (T_j^k - T_i^k - \tilde{t}_i - t_{ij}^k) - M(1 - x_{ij}^k) \qquad \forall k \in K, \forall (i,j) \in A^k : i,j \in N \tag{10}$$

When $x_{ij}^k = 1$, (10) captures slack between the actual service start at j and the earliest feasible arrival implied by service at i and transfer time. The EB-MD-VSP-TW further includes energy-consumption and charging constraints. Based on (Gkiotsalitis et al., 2023), constraints (11)–(17) are included.

$$\bar{e}_{o_k}^k = \phi_k \qquad \forall k \in K \tag{11}$$

$$\bar{e}_j^k = e_j^k - g_j^k \qquad \forall k \in K, \forall j \in V^k \cup F \tag{12}$$

$$e_j^k \leq (\bar{e}_i^k - \theta_{ij}) + M(1 - x_{ij}^k) \qquad \forall (i,j) \in A^k, \forall k \in K \tag{13}$$

$$e_j^k \geq (\bar{e}_i^k - \theta_{ij}) - M(1 - x_{ij}^k) \qquad \forall (i,j) \in A^k, \forall k \in K \tag{14}$$

$$g_i^k = \eta_i \qquad \forall i \in V^k, \forall k \in K \tag{15}$$

$$g_i^k = e_i^k - \phi_k^{max} \qquad \forall i \in F, \forall k \in K \tag{16}$$

$$\phi^{min} \leq e_j^k \qquad \forall k \in K \ \forall j \in V^k \cup F \cup \{d_k\} \tag{17}$$

Constraint (11) sets initial energy, (12) defines post-charging energy, (13)–(14) propagate energy across arcs, (15) fixes energy use at trip nodes, (16) implements the full-recharge rule at chargers, and (17) enforces the minimum SOC threshold. The equations introduced up to this point correspond to modeling components that are already available in the scientific literature. Starting with the next sub-section, the contributions of the current research are given.

Continuous-time reformulation of the EB-MD-VSP-TW

This work contributes to the literature in two ways. First, it presents a continuous-time reformulation of the EB-MD-VSP-TW. Second, it proposes a heuristic solution approach for the same problem. The present section focuses on the former contribution. To model charger utilization more realistically, the EB-MD-VSP-TW is reformulated in continuous time by explicitly modeling charging duration. We introduce the continuous variable τ_{kj} and constraints (18) and (19) for transitions from trip nodes $i \in V^k$ to charger nodes $j \in F$.

$$\tau_{kj} \geq \frac{\bar{e}_j^k - e_j^k}{CR} - M(1 - x_{ij}^k) \qquad \forall k \in K, \forall i \in V^k, \forall j \in F : (i,j) \in A^k \tag{18}$$

$$\tau_{kj} \leq \frac{\bar{e}_j^k - e_j^k}{CR} + M(1 - x_{ij}^k) \qquad \forall k \in K, \forall i \in V^k, \forall j \in F : (i,j) \in A^k \tag{19}$$

With τ_{kj} defined, the time-continuity constraint (5) is split by successor-node type. For non-charger successor nodes, continuity is enforced by (20).

$$T_j^k \geq T_i^k + \tilde{t}_i + t_{ij}^k - M(1 - x_{ij}^k) \qquad \forall k \in K, \forall (i,j) \in A^k : j \notin F \tag{20}$$

For charger successor nodes, time continuity is enforced by (21), which uses charging duration.

$$T_j^k \geq T_i^k + \tau_{ki} + t_{ij}^k - M(1 - x_{ij}^k) \qquad \forall k \in K, \forall (i,j) \in A^k : j \in F \tag{21}$$

To represent continuous-time charger occupation in the case study, we introduce the continuous completion-time variable CT_j^k and binary ordering variables $y_j^{k_1,k_2}$. These are used in (22)–(25) to define charging completion times, prevent overlap at shared chargers, and limit repeated charger visits.

$$CT_j^k \geq T_j^k + \frac{(\bar{e}_j^k - e_j^k)}{CR} - (1 - x_{ij}^k) \cdot M \qquad \forall k \in K, \forall i \in T, \forall j \in F \tag{22}$$

$$T_j^{k_1} \leq T_j^{k_2} + M \cdot y_j^{k_1,k_2} \qquad \forall j \in F, \forall k_1, k_2 \in K : k_1 \neq k_2 \tag{23}$$

$$T_j^{k_1} \geq CT_j^{k_2} + m + M(1 - y_j^{k_1,k_2}) \qquad \forall j \in F, \forall k_1, k_2 \in K : k_1 \neq k_2 \tag{24}$$

$$\sum_{(i,j) \in A^k : i \in V^k} x_{ij}^k \leq 1 \qquad \forall k \in K,\ \forall j \in F \tag{25}$$

Constraint (22) defines charging completion time, (23) and (24) impose pairwise charger sequencing, and (25) ensures each bus visits each charger at most once. To reflect depot capacity restrictions in the real-world setting, we add (26) and (27).

$$\sum_{j : (o_k, j) \in A_k} x_{o_k j}^k \ \leq \ 1 \qquad \forall k \in K \tag{26}$$

$$\sum_{j : (o_k, j) \in A_k} x_{o_k j}^k \leq p_m \qquad \forall m \in O \tag{27}$$

Constraint (26) limits each vehicle to at most one departure from its origin depot, while (27) enforces depot-level capacity p_m. Variable domains are completed by (28) and (29).

$$x_{ij}^k, y_j^{k_1,k_2} \in \{0,1\} \qquad \forall k \in K, \forall (i,j) \in A^k \tag{28}$$

$$w_{ij}^k, T_i^k, \tau_{kj}, CT_i^k \in R^+ \qquad \forall k \in K,\ \forall i \in N, \forall j \in F \tag{29}$$

The continuous-time reformulation therefore consists of objective function (9), and constraints (2)–(4), (6), (10), (11)–(17), (18)–(21), and (22)–(29).

Heuristic extension of the Continuous-time exact approach

Although the exact continuous-time EB-MD-VSP-TW can produce globally optimal solutions for small- and medium-scale instances, it becomes computationally expensive for large real-world schedules. To improve scalability while preserving modeling fidelity, we solve the formulation

sequentially across consecutive instances. When solving instance p, the terminal fleet state from instance $p-1$ (availability time, depot status, and battery level) is imposed as the initial condition. Because each solved instance under (2)–(4) starts and ends used vehicles at depots, the objective is extended to capture depot waiting and vehicle availability status across instances. Accordingly, we introduce the continuous variable wo_{ki} (origin-depot waiting time), the binary parameter bs_k (initial availability/full-battery status), and parameters $ST^k_{o_k}$, λ_2, and λ_3. The updated objective is given by (30).

$$\min \quad \sum_{k\in K}\sum_{(i,j)\in A^k} c^k_{ij}x^k_{ij} + \sum_{k\in K}\sum_{(i,j)\in A^k} \lambda_1 w^k_{ij} + \sum_{k\in K}\sum_{(o_k,j)\in A^k} \lambda_2 bs_k x^k_{o_k j} + \sum_{k\in K}\sum_{i\in o_k} \lambda_3 wo_{ki} \tag{30}$$

To activate these additions, constraints (31)–(33) are introduced.

$$T^k_j \le T^k_i + \tilde{t}_i + t^k_{ij} - M(1-x^k_{ij}) \qquad \forall k\in K, \forall (i,d_k)\in A^k \tag{31}$$

$$T^k_{o_k} \ge ST^k_{o_k} \qquad \forall k\in K \tag{32}$$

$$wo_{ki} \ge (1-bs_k)\left(T_{k,i} - ST^k_{o_k}\right) - M\left(1-x^k_{ij}\right) \qquad \forall k\in K, \forall (i,j)\in A^k \tag{33}$$

Constraint (31) fixes timing at final depot transitions when selected, (32) enforces earliest vehicle availability, and (33) activates origin waiting time only when relevant. The variable-domain constraint is correspondingly updated to (34).

$$w^k_{ij}, wo_{ki}, T^k_i, \tau_{kj}, CT^k_i \in R^+ \qquad \forall k\in K,\ \forall i\in N, \forall j\in F \tag{34}$$

With these final new parameters (λ_2, λ_3, $ST^k_{o_k}$, bs_k), decision variables (wo_{ki}), and constraints (31)-(34) in mind, the continuous time formulation of the EB-MD-VSP-TW consists of objective function (30), the vehicle-scheduling constraints (2)-(4), the classical time-windows constraint (6), the waiting time constraint (10), the energy-related constraints (11)-(17), and the revised time-continuity constraints (18)-(28) and constraints (31) to (34). Please note that the above formulation can be reduced to the one presented in the previous section , if λ_2, λ_3 and $ST^k_{o_k}$ are set to 0 ($\forall k \in K$) and if constraint (31) is relaxed. In Figure 2, one may notice a high-level representation how the extended exact model can be used in order to solve two EB-MD-VSP-TW sub-problems in a heuristic way.

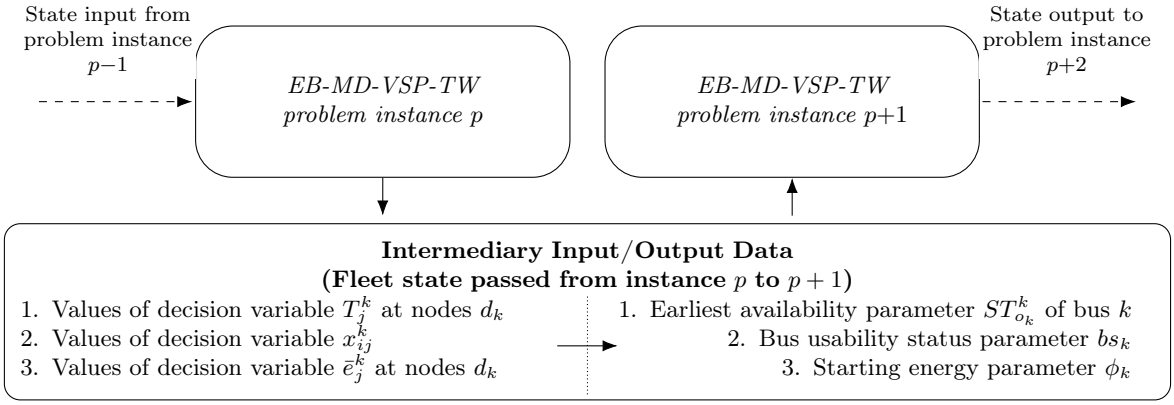


Figure 2: Conceptual representation of bus state transfer between two problem instances p and $p+1$.

Problem Decomposition and Solution through Bus Trips Clustering

As part of the proposed heuristic approach (formalized in Algorithm 1), we decompose the problem by clustering bus trips. This is done by partitioning the initial trip set using DBSCAN to reduce rolling-horizon subproblem size without modifying the EB-MD-VSP-TW formulation. Clustering is based on temporal proximity and deadheading distance (including direction-consistent chaining), so operationally related trips are grouped together, while noise trips are retained as singleton clusters. The clustering step constitutes only one component of the heuristic approach and does not, in itself, represent a standalone contribution of this study.

The heuristic is implemented as a stateful rolling-horizon procedure (Algorithm 1) for solving the EB-MD-VSP-TW. After clustering, trip groups are ordered by start time into batches, and the exact continuous-time EB-MD-VSP-TW model is solved sequentially at the cluster level within each batch. After each cluster solve, fleet availability times, state-of-charge values, and related state parameters are updated and propagated as initial conditions for subsequent clusters and batches. This preserves the dependence of later decisions on earlier charging and assignment choices while substantially reducing computational burden relative to solving the full-day instance in a single run.

Algorithm 1 Stateful Rolling-Horizon Solution of the EB-MD-VSP-TW Model

Input: Bus trip schedules, fleet specification, depot and charging infrastructure data, clustering parameters.

Output: Feasible and optimized bus blocks schedule and final state of the bus fleet.

```
Apply a clustering method to the daily bus trip schedule
Sort clusters in ascending order of starting time
Initialize fleet availability times and state-of-charge values
Initialize cumulative objective value
for each cluster in all clusters do
    Solve the exact EB-MD-VSP-TW model for the current cluster
    if the model is infeasible then
        Terminate and return infeasibility
    end if
    Extract optimal vehicle schedules for the cluster
    Update fleet availability times and state-of-charge values
    Accumulate objective contribution of the cluster
end for
Return: Final fleet state and cumulative objective value
```

3 Results and discussion

All MILP models and solution approaches tested in this results section have been implemented in Python 3.13.9 and Gurobi solver version 13.0. Computation for this section relied on a Lenovo ThinkSystem ST250 server (Intel Xeon E-2356G, 64 GB RAM).

Testing on replicable synthetic EB-MD-VSP-TW instances

In this section, the proposed exact continuous-time MILP model is applied to reproducible EB-MD-VSP-TW instances, which are openly available online (Gkiotsalitis et al., 2023). Due to space limitations, in Table 1 of this conference paper we include only results for the largest available synthetic instances (30 trips).

Table 1: Results for 30-trip instances when solving with exact model. SP: Solution Performance, LB: Lower Bound, LBG: Gap between the solution and the Lower Bound, OG: Optimality Gap, CPT: Computation time (s).

	Solution Information				
Instance	SP	LB	LBG	OG	CPT (s)
$D2_S3_C30_a$	5819.40	5533.64	4.91	4.91	18000.03
$D2_S3_C30_b$	5548.02	5548.02	0.00	0.00	1024.50
$D2_S3_C30_c$	4002.69	4002.69	0.00	0.00	1591.52
$D2_S3_C30_d$	4895.04	4895.04	0.00	0.00	916.62
$D2_S3_C30_e$	5777.74	5777.74	0.00	0.00	360.80
Average	-	-	-	-	4378.69

The exact model remains effective for most instances at this scale. Four of the five instances are solved to proven optimality, with zero optimality gap and identical solution performance (SP) and lower bound (LB) values. For instance $D2_S3_C30_a$, the solver reaches the 5-hour time limit

and terminates with a 4.91% optimality gap. However, the incumbent solution remains close to the lower bound (SP = 5819.40, LB = 5533.64), indicating good solution quality despite incomplete convergence. Computation times vary substantially, ranging from 360.80 to 18,000.03 seconds, with an average of 4,378.69 seconds. This reflects the significant computational effort required for exact solution of 30-trip instances. Overall, Table 1 highlights the practical limits of the exact model on larger EB-MD-VSP-TW instances. Although most instances are solved optimally, the time-limited run and high runtime variability motivate alternative approaches, such as heuristic or hybrid methods, for larger cases.

Table 2 summarizes the outcomes for the 30-trip instances, when solved with the proposed heuristic approach. Unlike the exact model (results reported in Table 1), the heuristic decomposes each instance into smaller clusters (as described in Section 2), solves them independently, and aggregates the partial solutions to obtain a complete schedule. At the cluster level, all subproblems are solved to proven optimality, as indicated by zero optimality gaps and identical values of solution performance (SP) and lower bound (LB) for all cluster rows in Table 2. For the aggregated per-instance heuristic solutions (rows labeled `_total`), no global lower bound is reported, and thus no optimality gap is provided. As expected, these aggregated heuristic solutions are not globally optimal with respect to the original 30-trip instances (objective function values calculated by the exact approach are lower than the ones calculated by the heuristic across all available instances).

Table 2: Results for 30-trip instances when using the heuristic approach.

	Solution Information				
Instance	SP	LB	LBG	OG	CPT (s)
D2_S3_C30_a_cluster_0	2635.71	2635.71	0.00	0.00	46.37
D2_S3_C30_a_cluster_1	3493.19	3493.19	0.00	0.00	3.80
D2_S3_C30_a_total	6128.91	-	-	-	50.17
D2_S3_C30_b_cluster_0	2731.73	2731.73	0.00	0.00	17.68
D2_S3_C30_b_cluster_1	3353.32	3353.32	0.00	0.00	9.48
D2_S3_C30_b_total	6085.05	-	-	-	27.16
D2_S3_C30_c_cluster_0	2117.48	2117.48	0.00	0.00	3.28
D2_S3_C30_c_cluster_1	2212.17	2212.17	0.00	0.00	1.36
D2_S3_C30_c_total	4329.65	-	-	-	4.65
D2_S3_C30_d_cluster_0	3420.55	3420.55	0.00	0.00	5.76
D2_S3_C30_d_cluster_1	1956.11	1956.11	0.00	0.00	3.34
D2_S3_C30_d_total	5376.66	-	-	-	9.10
D2_S3_C30_e_cluster_0	3071.31	3071.31	0.00	0.00	7.35
D2_S3_C30_e_cluster_1	3044.63	3044.63	0.00	0.00	1.30
D2_S3_C30_e_total	6115.94	-	-	-	8.65
Average	-	-	-	-	9.97

Relative to the exact approach, computation times are substantially reduced. Cluster-level runtimes range from 1.30 to 46.37 seconds, and total heuristic runtime per 30-trip instance ranges from 4.65 to 50.17 seconds. Table 3 shows per-instance time reductions between 97.35% and 99.72%. The heuristic SP is higher than the exact SP in all five instances, with gaps from 5.32% to 9.84% (average: 7.77%). Despite this loss in solution quality, average computation time decreases from 4,378.69 seconds (exact) to 19.95 seconds (heuristic), a 98.67% reduction. Overall, the heuristic substantially reduces computational burden while producing high-quality feasible solutions, albeit without global optimality guarantees.

Table 3: Per-instance solution performance comparison between exact and heuristic approaches (optimality gap and computation time).

Instance	SP_{exact}	SP_{heur}	Gap (%)	CPT_{exact} (s)	CPT_{heur} (s)	Time reduction (%)
D2_S3_C30_a	5819.40	6128.91	5.32	18000.03	50.17	99.72
D2_S3_C30_b	5548.02	6085.05	9.68	1024.50	27.16	97.35
D2_S3_C30_c	4002.69	4329.65	8.17	1591.52	4.65	99.71
D2_S3_C30_d	4895.04	5376.66	9.84	916.62	9.10	99.01
D2_S3_C30_e	5777.74	6115.94	5.85	360.80	8.65	97.6
Average	-	-	7.77	4378.69	19.95	98.67

Comparing the Heuristic and Exact Approach on a Small-scale Case Study

This section applies the exact and heuristic approaches to real-world instances based on the Athens Urban Transport Organization (OASA) network. The selected lines (217, 229, B1, and 831) are currently operated with conventional buses and are candidates for electrification. The proposed model supports ex ante assessment of electrification requirements, including fleet size, waiting times, and traversal-related costs. Lines 217 and 831 are shown in Figures 3 and 4.

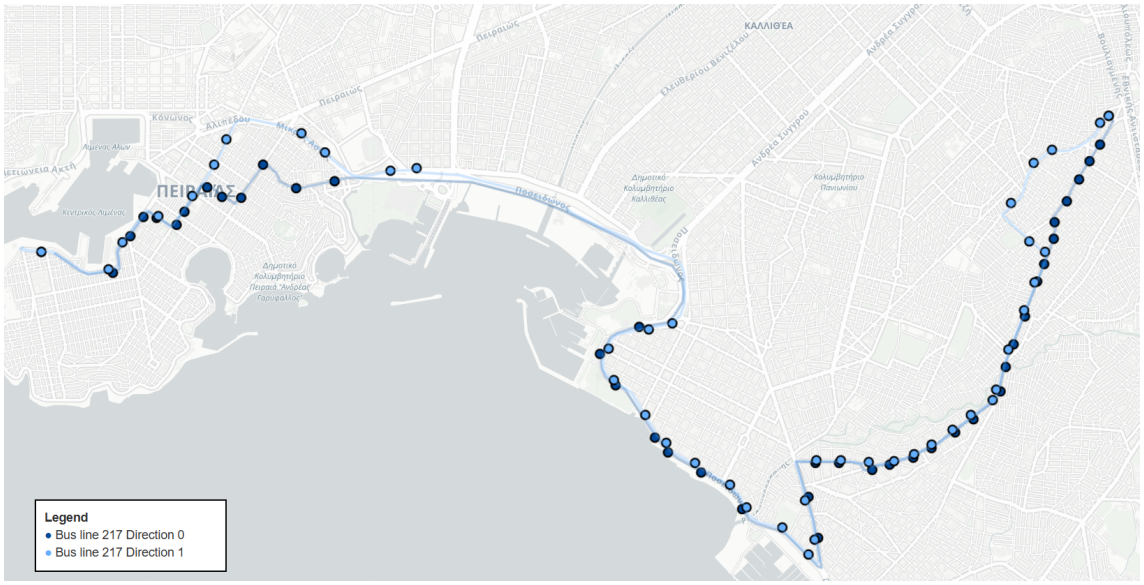


Figure 3: Bus line 217.

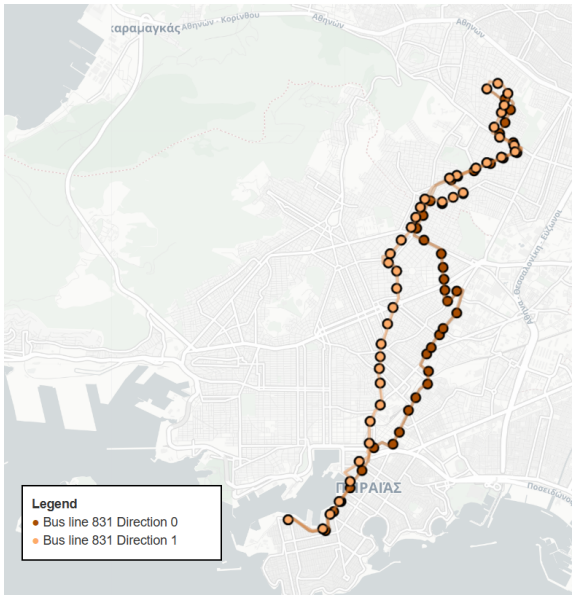


Figure 4: Bus line 831.

For the Athens case study, we set $c_{ij} = 5$, $\lambda_1 = 8$, $\lambda_2 = 150$, and $\lambda_3 = 0.5$. Vehicle blocks may start from O_1 or O_2, all vehicles depart with full battery ($\phi_k = 350.0$ kWh), and battery levels must remain above $\phi^{\min} = 100.0$ kWh. Each block ends at the corresponding depot-in node (D_1 or D_2). For the selected initial trips subset, the first three trips in each direction of the considered lines are used.

Table 4 reports the exact solution for the 24-trip EB-MD-VSP-TW instance in compact horizontal form (node sequences, arrival times, E_{pre}, and E_{bar}). The exact model covers all 24 services using six vehicles (four from Depot 1 and two from Depot 2). Two charging events occur at C_1: $D1_V2$ charges at time 720.65 (from $E_{\text{pre}} = 125.4$ to $E_{\text{bar}} = 350.0$) before T_9, and $D2_V1$ charges at

time 367.32 (from $E_{\text{pre}} = 306.8$ to $E_{\text{bar}} = 350.0$) before T_{10}. The exact model attains an objective value of 1,427.33 in 250.24 seconds. Overall, Table 4 shows that the exact approach jointly handles routing, scheduling, and battery management across multiple depots while maintaining time and energy feasibility and full service coverage.

Table 4: Vehicle schedules for the 24-trip EB-MD-VSP-TW instance (exact approach), objective value = 1,427.33. For each vehicle, the node sequence is reported horizontally, followed by the corresponding arrival times, pre-service energy levels (E_{pre}), and post-node battery levels (E_{bar}).

Vehicle ID	**Field**	**Values (in node-sequence order)**
$D1_V1$	Node sequence	$O_1 \to T_4 \to T_2 \to T_5 \to T_{14} \to T_{18} \to T_{15} \to D_1$
	Arr. Time	336.02, 341.67, 400.00, 451.67, 524.33, 596.67, 670.00, 758.46
	E_{pre}	−, 345.1, 314.7, 286.4, 256.0, 216.9, 175.9, 122.8
	E_{bar}	350.0, 314.7, 286.4, 256.0, 216.9, 175.9, 136.8, −
$D1_V2$	Node sequence	$O_1 \to T_{16} \to T_{13} \to T_{17} \to T_7 \to T_6 \to T_8 \to C_1 \to T_9 \to D_1$
	Arr. Time	283.21, 299.33, 372.67, 445.00, 535.00, 595.00, 655.00, 720.65, 810.00, 875.65
	E_{pre}	−, 336.0, 295.0, 255.9, 214.9, 187.8, 157.4, 125.4, 334.8, 302.7
	E_{bar}	350.0, 295.0, 255.9, 214.9, 187.8, 157.4, 130.3, 350.0, 307.6, −
$D1_V3$	Node sequence	$O_1 \to T_{12} \to D_1$
	Arr. Time	1244.34, 1250.00, 1321.58
	E_{pre}	−, 345.1, 301.6
	E_{bar}	350.0, 316.8, −
$D1_V4$	Node sequence	$O_1 \to T_{11} \to T_3 \to D_1$
	Arr. Time	990.34, 996.00, 1050.00, 1107.32
	E_{pre}	−, 345.1, 316.8, 283.6
	E_{bar}	350.0, 316.8, 288.5, −
$D2_V1$	Node sequence	$O_2 \to T_1 \to C_1 \to T_{10} \to D_2$
	Arr. Time	298.49, 310.00, 367.32, 387.38, 452.89
	E_{pre}	−, 340.0, 306.8, 345.1, 306.8
	E_{bar}	350.0, 311.7, 350.0, 316.8, −
$D2_V4$	Node sequence	$O_2 \to T_{19} \to T_{22} \to T_{20} \to T_{23} \to T_{21} \to T_{24} \to D_2$
	Arr. Time	298.17, 309.68, 353.34, 405.00, 449.68, 501.33, 545.00, 608.17
	E_{pre}	−, 340.0, 318.0, 297.3, 275.3, 254.7, 232.6, 202.0
	E_{bar}	350.0, 318.0, 297.3, 275.3, 254.7, 232.6, 212.0, −

Table 5 reports the heuristic solution for the same 24-trip instance. As in the exact approach, all 24 services are covered, but the heuristic constructs seven vehicle blocks using five vehicles by allowing multiple disjoint duties for the same vehicle (heuristic approach allows multiple blocks for the same vehicle, whereas exact approach does not). This occurs for $D1_V1$ and $D1_V5$, each of which operates two duties. As in the exact solution, blocks start at depot-out nodes and end at the corresponding depot-in nodes. First duties start fully charged ($\phi_k = 350.0$), whereas later duties may inherit residual energy (e.g., $E_{\text{bar}} = 155.9$ for the second duty of $D1_V1$ and 311.3 for the second duty of $D1_V5$). Battery levels remain above $\phi^{\min} = 100.0$ throughout.

Two charging events occur at C_1: $D1_V1$ charges at time 875.66 (with $E_{\text{pre}} = 117.2$) before T_{22}, and $D2_V4$ charges at time 368.20 (with $E_{\text{pre}} = 316.6$) before T_{20}; in both cases, charging restores E_{bar} to 350.0. The heuristic attains an objective value of 1,536.6, compared with 1,427.33 for the exact solution, corresponding to a relative gap of 7.66%. This illustrates the expected trade-off between solution quality and computational tractability.

Overall, Table 5 shows that the heuristic approach produces time-feasible and energy-feasible schedules that cover all transport services, while relying on the added flexibility of multiple disjoint duties for the same vehicle (here, $D1_V1$ and $D1_V5$), unlike the exact formulation.

Table 5: Vehicle schedules for the 24-trip EB-MD-VSP-TW instance (heuristic approach), objective value = 1,536.6.

Vehicle ID	**Field**	**Values (in node-sequence order)**
$D1_V1$	Node sequence	$O_1 \to T_4 \to T_1 \to T_5 \to T_2 \to T_6 \to T_3 \to D_1$
	Arr. Time	283.21, 299.33, 372.67, 445.00, 518.33, 590.67, 670.00, 758.46

Continued on next page

Vehicle ID	Field	Values (in node-sequence order)
	E_{pre}	$-$, 336.0, 308.3, 280.6, 252.9, 225.2, 197.5, 155.9
	E_{bar}	350.0, 308.3, 280.6, 252.9, 225.2, 197.5, 169.8, $-$
$D1_V1$	Node sequence	$O_1 \to T_{21} \to C_1 \to T_{22} \to D_1$
	Arr. Time	792.42, 810.00, 875.66, 985.00, 1056.58
	E_{pre}	$-$, 140.6, 117.2, 345.1, 311.3
	E_{bar}	155.9, 122.1, 350.0, 326.5, $-$
$D1_V3$	Node sequence	$O_1 \to T_{15} \to T_{14} \to T_{16} \to T_{18} \to T_{17} \to T_{19} \to D_1$
	Arr. Time	336.02, 341.67, 400.00, 455.00, 535.00, 595.00, 655.00, 720.66
	E_{pre}	$-$, 345.1, 326.5, 308.0, 289.4, 270.9, 252.3, 228.9
	E_{bar}	350.0, 326.5, 308.0, 289.4, 270.9, 252.3, 233.8, $-$
$D1_V5$	Node sequence	$O_1 \to T_{23} \to D_1$
	Arr. Time	1032.42, 1050.00, 1107.32
	E_{pre}	$-$, 334.8, 311.3
	E_{bar}	350.0, 316.2, $-$
$D1_V5$	Node sequence	$O_1 \to T_{24} \to D_1$
	Arr. Time	1244.34, 1250.00, 1321.58
	E_{pre}	$-$, 306.4, 272.6
	E_{bar}	311.3, 287.8, $-$
$D2_V4$	Node sequence	$O_2 \to T_{13} \to C_1 \to T_{20} \to D_2$
	Arr. Time	298.49, 310.00, 368.20, 385.00, 450.51
	E_{pre}	$-$, 340.0, 316.6, 345.1, 316.6
	E_{bar}	350.0, 321.5, 350.0, 326.5, $-$
$D2_V5$	Node sequence	$O_2 \to T_7 \to T_{10} \to T_8 \to T_{11} \to T_9 \to T_{12} \to D_2$
	Arr. Time	298.17, 309.68, 353.34, 405.00, 448.67, 501.33, 545.00, 608.17
	E_{pre}	$-$, 340.0, 324.3, 308.7, 293.0, 277.3, 261.6, 236.0
	E_{bar}	350.0, 324.3, 308.7, 293.0, 277.3, 261.6, 246.0, $-$

4 Conclusions

This paper addressed tactical electric bus scheduling via the EB-MD-VSP-TW in continuous time. The formulation improves charger-use fidelity over discrete-time approximations while preserving implementable schedules under depot, time-window, and battery constraints. Because the exact model is computationally demanding on larger instances, a stateful rolling-horizon heuristic was developed to improve scalability.

The proposed methods were evaluated on synthetic benchmark instances and real-world bus lines in Athens, Greece. The results indicate that continuous-time charging provides a more realistic representation of charger occupation while supporting feasible scheduling decisions, whereas the heuristic offers a computationally tractable alternative for larger instances. Ongoing work investigates stronger decomposition approaches for instances with up to 200 trips; although preliminary, these results will be presented at the conference.

Acknowledgements

The present work is partially funded by the metaCCAZE Project (Flexibly adapted MetaInnovations, use cases, collaborative business and governance models to accelerate deployment of smart and shared Zero Emission mobility for passengers and freight). This project has received funding from the European Union's Horizon Europe research and innovation programme under grant agreement No. 101139678

References

Bodin, L. D. (1990). Twenty years of routing and scheduling. *Operations Research*, *38*(4), 571–579.

Carpaneto, G., Dell'amico, M., Fischetti, M., & Toth, P. (1989). A branch and bound algorithm for the multiple depot vehicle scheduling problem. *Networks*, *19*(5), 531-548.

Davatgari, A., Verbas, O., Cokyasar, T., & Mohammadian, A. K. (2024). Optimization of electric bus scheduling and charger location. *Procedia Computer Science*, *238*, 361-368. (The 15th International Conference on Ambient Systems, Networks and Technologies Networks (ANT) / The 7th International Conference on Emerging Data and Industry 4.0 (EDI40), April 23-25, 2024, Hasselt University, Belgium)

Desaulniers, G., Lavigne, J., & Soumis, F. (1998). Multi-depot vehicle scheduling problems with time windows and waiting costs. *European Journal of Operational Research*, *111*(3), 479-494.

Eliiyi, D. T., Ornek, A., & Karakütük, S. S. (2009). A vehicle scheduling problem with fixed trips and time limitations. *International Journal of Production Economics*, *117*(1), 150–161.

Gerbaux, J., Desaulniers, G., & Cappart, Q. (2025). A machine-learning-based column generation heuristic for electric bus scheduling. *Computers & Operations Research*, *173*, 106848.

Gkiotsalitis, K., Iliopoulou, C., & Kepaptsoglou, K. (2023). An exact approach for the multi-depot electric bus scheduling problem with time windows. *European Journal of Operational Research*, *306*(1), 189–206.

Jiang, Y., & He, T. (2022). Optimal charging scheduling and management with bus-driver-trip assignment considering mealtime windows for an electric bus line. *Complexity*, *2022*, 3087279.

Lipman, T. E. (2025, Jun 16). Recent developments and challenges with electric bus implementation for transit fleets. *Current Sustainable/Renewable Energy Reports*, *12*(1), 19.

Lu, C., Xie, D.-F., Zhao, X.-M., & Qu, X. (2023). The role of alternative fuel buses in the transition period of public transport electrification in europe: a lifecycle perspective. *International Journal of Sustainable Transportation*, *17*(6), 626–638.

Orloff, C. S. (1976). Route constrained fleet scheduling. *Transportation Science*, *10*(2), 149–168.

Pelletier, S., Jabali, O., Mendoza, J. E., & Laporte, G. (2019). The electric bus fleet transition problem. *Transportation Research Part C: Emerging Technologies*, *109*, 174-193.

Rogge, K. S., & Goedeking, N. (2024, mar). Challenges in accelerating net-zero transitions: insights from transport electrification in germany and california. *Environmental Research Letters*, *19*(4), 044007.

Wang, C., Guo, C., & Zuo, X. (2021). Solving multi-depot electric vehicle scheduling problem by column generation and genetic algorithm. *Applied Soft Computing*, *112*, 107774.

Yao, E., Liu, T., Lu, T., & Yang, Y. (2020). Optimization of electric vehicle scheduling with multiple vehicle types in public transport. *Sustainable Cities and Society*, *52*, 101862.